Surface elastic waves in granular media under gravity and their relation to booming avalanches

L. Bonneau, B. Andreotti, and E. Clément
Laboratoire de Physique et Mécanique des Milieux Hétérogènes associé au CNRS (UMR 7636) et aux Universités Paris 6 et Paris 7, 10 rue Vauquelin, 75005 Paris, France

(Received 25 January 2006; revised manuscript received 26 September 2006; published 8 January 2007)

Due to the nonlinearity of Hertzian contacts, the speed of sound c in granular matter is expected to increase with pressure as $P^{1/6}$. A static layer of grains under gravity is thus stratified so that the bulk waves are refracted toward the surface. The reflection at the surface being total, there is a discrete number of modes (both in the sagittal plane and transverse to it) localized close to the free surface. The shape of these modes and the corresponding dispersion relation are investigated in the framework of an elastic description taking into account the main features of granular matter: Nonlinearity between stress and strain and the existence of a yield transition. We show in this context that the surface modes localized at the free surface exhibit a waveguide effect related to the nonlinear Hertz contact. Recent results about the song of dunes are reinterpreted in light of the theoretical results. The predicted propagation speed is compared with measurements performed in the field. Taking into account the finite depth effects, we show that the booming instability threshold can be explained quantitatively by a waveguide cutoff frequency below which no sound can propagate. Therefore, we propose another look at a recent controversy, confirming that the song of dunes can well originate from a coupling between avalanching grains and surface elastic waves once the specificity of surface waves (we baptized Rayleigh-Hertz) is correctly taken into account.

DOI: 10.1103/PhysRevE.75.016602 PACS number(s): 46.40.−f, 81.05.Rm

I. INTRODUCTION

From the physical point of view, surface waves in an elastic material (called Rayleigh waves) are a combination of compression and shear waves that are traveling at speeds slightly smaller than bulk shear waves [1]. Nevertheless, in the context of granular matter, the propagation of waves close to the surface of a sand bed has risen the most contradictory claims. If we exclude the recent suggestion [2] of a compressibility originating from an interstitial fluid, it is well accepted that sound in sand propagates through the grains contact—the so-called elastic skeleton. A simple (mean-field) argument shows that, under these conditions, bulk waves cannot propagate parallel to the surface. This is due to the increase of material stiffness [3] with depth which should redirect the wave front toward the free surface (mirage effect). Arguing that the free surface absorbs the wave (we will see that this is actually not the case), Liu and Nagel [4] concluded that elasticlike modes cannot exist at all in granular media under gravity. Their experiments have shown a nonharmonic response of the system, related to an extreme sensitivity of the acoustic signal to minute local reorganizations. This was ascribed later to the speckle effect [5], a dominant feature for probe sizes on the order of one grain. In the context of physics, the very existence of such waves and their ability to propagate over large distances has remained problematic. However, the propagation of sound at the surface of sand was evidenced and characterized in two other contexts: the localization of preys by scorpions and the spontaneous emission of sound by sand avalanches (the so-called song of dunes). As it is an important justification for the present work, we would like to recall the state of the art and the open questions about these two issues.

Prey detection of scorpions. To our knowledge, the first experiments on wave propagations over sandy free surfaces were conducted in a biological context. Some desert animals like scorpions are blind—they mostly live at night—and use sand-born surface sound waves up to a distance of half a meter in order to localize their prey [6]. On each of their legs they possess slit sensilla receptors and associated neural connections, such as to detect small phase lags and orient their killing jump very efficiently. Biologists like Ph. Brownell and his collaborators [6] have identified surface propagation of sound and measured a rather low speed ($c \simeq 50$ m/s in the 100–500 Hz range) compatible with the animal biological capacities for signal processing [7]. From the physical point of view, puzzling questions remain to understand the true nature of these waves and it is the aim of the article to help clarify the issue. Nevertheless, an intriguing question remains. It has been shown recently, in model systems, that localized modes of vibration with a complex spatial structure do exist as a signature of the disordered nature of the material [8,9]. In the limit of vanishing confining pressure (at a surface, for example), their spatial extention could in principle be very large. From a biological point of view, knowing that the scorpion legs are only a few grains in size, it would be crucial to understand to what extent the ability to detect precisely the location of a sound emission locus (a long wavelength traveling wave) could be influenced by other complex spatial modes. This precise issue is out of the scope of the present article but remains in our mind a vivid background problem.

The song of dunes. Many sand dunes spontaneously make loud booming noises when they avalanche [10]. Records of the sound are centuries old [11–15], but the cause has remained a mystery until recently [16–18]. Surface elastic waves were recently found to be fundamental in the song of dunes phenomenon [19]. By an extensive characterization of the phenomenon in the field, one of us [19] has shown that (i) the sound emitted in the air is not due directly to the avalanche but to the coherent vibration of the free surface (surface elastic modes); (ii) these surface waves exist both

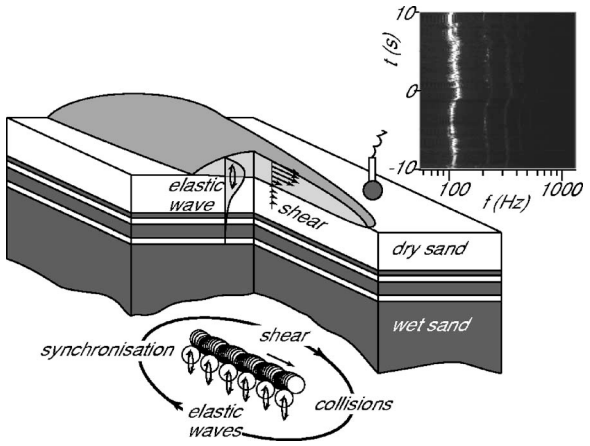

FIG. 1. Schematic of a booming avalanche flowing along the slip face of a dune. The grains are submitted to both pressurelike elastic waves and to shear localized at the interface between the flowing layer and the static sand bed. The emission in the air is due to the vibration of the free surface, which acts as a loudspeaker. In the inset, we display a sonogram from a probe downhill the avalanche triggering place. This demonstrates that the emission frequency is well defined when the avalanche is homogeneous. It also shows that the free surface vibrates both in the avalanche ($t>0$) and outside, in the static zone ($t<0$). No discontinuity (in frequency and amplitude) is observed at $t=0$, when the avalanche front reaches the position at which the sound is recorded (very close to the soil). The instability results from an interaction between the shear deformations and the elastic waves: The collisions excite the elastic waves that in turn tend to synchronize them. The stability or instability of this locking mechanism is a matter of probability for the granular collisions to act in phase with the acoustic wave.

inside and outside the avalanche and are indeed localized at few centimeters below the surface; (iii) the emission frequency f is controlled by the velocity gradient inside the avalanche shear layer, which is also the collision rate of the rolling grains, and not by any resonant condition; (iv) for a gravity induced flow, f is roughly equal to $\simeq 0.4\sqrt{g/d}$, where g is the gravity and d the grain size; (v) the upper bound of the sound level ($\simeq$105 dB) corresponds to the amplitude of vibration for which the normal acceleration of the free surface just balances gravity, i.e., whenever the grains start taking off the surface; (vi) the elastic surface waves tend to synchronize the grains collisions; (vii) the elastic surface waves propagate at a speed of the same order of magnitude ($\simeq$40 m/s at 100 Hz) at the surface of a static sand bed and of a flowing layer. (See Fig. 1.)

This series of facts point toward a precise mechanism involving the interaction between the collisions inside the avalanche and the elastic modes [19]. During an avalanche, there are two distinct modes of deformation. On one hand, the grains move one with respect to the others (shearing); on the other hand, they remain in contact with their neighbors so that pressure waves can propagate through the (sheared) elastic skeleton. During a collision between two grains, part of the kinetic energy is dissipated but part is transferred through the grains deformation into elastic waves—both surface waves and localized modes. Of course, in a silent avalanche, the grain motion is not correlated at long distance so that the contributions of different collisions to the coherent modes interfere destructively. The key point of the mechanism proposed in [19] is the demonstration on a simple model that coherent elastic waves tend to synchronize the collisions of the grains. This suggests that the song of dunes originates from a wave particle mode locking. The reference state in which the collisions are randomly distributed becomes unstable toward a mode in which a propagative coherent elastic mode is excited and, simultaneously, a fraction of the moving grains gets synchronized. This mode increases in amplitude since the wave synchronizes the collisions which in turn excite the wave constructively. The only condition of instability is that sufficient energy may be transferred from translation to vibration, and of course that elastic surface waves can propagate. We shall return later on to this last condition.

Independent measurements of "*the*" sound propagation speed at the surface of Californian booming dunes were performed by Hunt *et al.* [20] with a hammer hitting a metallic plate, giving $c\simeq 210$ m/s. On this basis, they supported the (old) idea according to which booming avalanches simply come from a resonance inside the dune. Recently, booming sand flows were reproduced in the lab by Douady *et al.* [21] by inducing a small scale avalanche of size H with a blade moving at a controlled velocity V. The emission frequency f increases with V/H and gives back the value measured in the field for asymptotically small velocities or large avalanches [see Fig. 9(b) of the present paper reproducing experimental data]. This shows that there is no need to have a large dune (a large resonant cavity) below the avalanche for the phenomenon to exist. The second original point of the paper is the evidence of a threshold for the booming instability, which depends in a complex manner on V and on H [see Fig. 9(a)]. On this basis, Douady *et al.* challenged the existence and the role of surface elastic modes [19] and gave a (slightly) different explanation: "Coupling (shear?) waves" would propagate at $c\simeq 0.94$ m/s across the avalanche and synchronize the flow. Note that is indeed very low sound speed, which has never been observed directly in the context of granular matter. In particular, depending on different authors, the propagation speed would be between 1 m/s (estimated from an instability threshold [21]) and 210 m/s (directly measured by impact [20]), with an intermediate value $\simeq$40 m/s (directly measured at 100 Hz with a sinusoidal source [19]). In summary, if it is now clear that acoustic waves are involved in the song of dunes, their exact nature is still controversial.

Importantly, it is now beyond any doubt that no resonance at the scale of a dune is necessary for the phenomenon to occur: The same flow on different resonant cavities (e.g., different dune sizes) produce the same frequency and different flows on the same resonant cavity (e.g., the surface of the same dune) produce different frequencies. The controversy on this subject mainly results from the way avalanches were produced on the dune slip faces. Most people spontaneously generate inhomogeneous intermittent avalanches by beating the legs like scissors [20], which results in important variations in emission frequency. However, a uniform pushing is needed to obtain homogeneous avalanches, controlled by gravity [19,21].

A direct motivation of the present paper is to provide a theoretical framework for wave propagation at the surface of

a sand bed under gravity. Do the surface modes exist? What is their dispersion relation? What is the expected propagation speed? Can the booming instability threshold [21] be conciliated with the directly observed surface elastic waves [19]? What is the role, if any, of the resonant cavity below the avalanche?

Sound in sand under strong compression. Granular matter, as a collection of stiff grains under moderate confining pressure, bears intergranular contact surfaces of a scale much smaller than a typical grain size. In fact, the surfaces and the orientations of contacts are likely to be modified either reversibly or irreversibly under the variation of intergranular forces. This feature is at the origin of many inherent difficulties when one wishes to determine the macroscopic constitutive properties. Moreover, the packing topology which determines the contact geometry is usually of a strongly disordered nature [22] and average quantities like deformation fields are quite subtle to define [23]. Thus, already at the most simple level of description, involving local nonlinear elastic relations (the classical Hertz force problem [3]), a mean-field approach which identifies the local granular displacements with macroscopic deformations, is failing quantitatively [24–29]. In the context of physics, tests were mostly made using sound wave bulk propagation [5,24,28,29] under rather large confining pressures P and results show a propagation velocity $c \propto P^{1/4}$ instead of the standard mean-field prediction $c \propto P^{1/6}$. Actually, Makse *et al.* [29] have shown clearly using numerical simulations that if one takes into account the effective increase of the number of contacts with pressure, the agreement is bettered (especially for compression waves). Nevertheless, an essential discrepancy still lies in the assessment of the shearing stiffness merging from local tangential contact forces [29]. Note also that, from an experimental point of view, the exact origin of the discrepancy is not totally clear [30]. Other features such as angular shape contacts [31] or the existence of a soft layer surrounding the grains [32] can modify the propagation velocities in directions observed experimentally.

In the limit of vanishing confining pressure very few results on sound wave propagation exist either experimentally [4,6,19] or theoretically [33]. In this paper, we address the issue of surface wave propagation in the theoretical framework of continuous nonlinear elasticity. The model we use was recently introduced by Jiang and Liu [34] to describe granular constitutive properties. In the first part of this paper, we give a short state of the art concerning the elastic description of granular media in the static phase and present the phenomenology introduced by Jiang and Liu. In the second part, we show the existence of surface waves in a semi-infinite slab of grains under gravity. We derive the shape of the modes and their dispersion relation. In the third part, we turn to the song of dunes problem and compare the theoretical dispersion relation to experimental measurements made in the field. We also show that the booming instability threshold can be reproduced quantitatively if finite depth effects (Appendices B and C) are taken into account and simply comes from a waveguide cutoff.

II. THE JIANG-LIU MODEL

A. Strain-stress relation

We introduce the displacement field $\rho\mathbf{U}$ and the stress tensor σ_{ij}. With our conventions, the dynamical equation reads

$$\rho\ddot{\mathbf{U}} = -\nabla\bar{\sigma} + \rho\mathbf{g}. \tag{1}$$

To relate the stress tensor σ_{ij} to the strain tensor $u_{ij}=(1/2)\times(\partial U_i/\partial x_j+\partial U_j/\partial x_i)$, Jiang and Liu have recently proposed a phenomenological formulation based on a simple energetic formulation:

$$F_{el} = E\delta^{1/2}\left(\frac{2}{5}\mathcal{B}u_{ll}\delta^2 + \mathcal{A}u_s^2\right), \tag{2}$$

where E is the material Young's modulus and $\mathcal{A}$ and $\mathcal{B}$ are two dimensionless numbers. The volumic compression is

$$\delta = -\mathrm{Tr}(u_{ij}), \tag{3}$$

$u_{ij}^0=u_{ij}+(\delta/3)\delta_{ij}$ is the traceless strain tensor, and

$$u_s^2 = u_{ij}^0 u_{ij}^0$$

is its modulus squared. The derivation of the stress tensor yields

$$\sigma_{ij} = E\sqrt{\delta}\left(\mathcal{B}\delta\delta_{ij} - 2\mathcal{A}u_{ij}^0 + \frac{\mathcal{A}u_s^2\delta_{ij}}{2\delta}\right). \tag{4}$$

Interestingly, the last term of this equation, $\mathcal{A}u_s^2\delta_{ij}/2\delta$, does not exist in standard Boussinesq nonlinear elasticity [35]. This discrepancy comes from the fact that this last theory is not derived from an elastic potential, contrary to the Jiang-Liu model. This fundamental question is also a strong motivation to put under clear experimental test the propagation of elastic waves in granular assemblies. It is important to note that this elegant and compact formulation of elastic energy is able to reproduce many qualitative features observed experimentally, such as the existence of a Coulomb-like failure or stress-induced anisotropy. Efforts have been made by the authors to compare quantitatively their model to the output of several experimental measurements, such as systematic triaxial tests, the response to a local load, and static equilibrium in a column. The agreement was noticeable, especially in view of the minimal amount of free parameters in the model. The possibility to follow the elastic behavior up to the limit of failure is also a promising feature of the model in the context of slope stability monitored by sound waves. This feature is quite original if one compares to the standard Boussinesq nonlinear elasticity framework [35]. Of course, issues like irreversible deformation fields (plasticity) are still questionable in the framework of this model; nevertheless, it provides a well defined starting point for a complete analysis and modeling of elastic vibrations. Furthermore, this approach can be generalized easily with a power law not representing necessarily the Hertzian interaction. Thus one could, in principle, take into account the existence of other types of nonlinear contact force laws [31,32]. In the present paper, we will limit ourselves to Hertzian interactions and we

will derive sound propagation around the simplest possible reference state.

B. Mean field determination of the compression modulus

Since Mindlin in the 1950s, several works, focusing on sound wave bulk propagation in granular materials, have derived from local Hertzian interactions, the effective elastic moduli [24–27]; for a recent and clear review, see Makse *et al.* [29] and references therein. We just recall here the mean-field results for a packing of spheres of compacity Φ and an average coordination number Z. First let us write the interparticular forces between two spheres of radii R_1 and R_2 and half overlap $\xi=1/2(R_1+R_2-|\vec{x}_1-\vec{x}_2|)$, $R=2R_1R_2/(R_1+R_2)$ (if $R_1=R_2$, R is the sphere radius). The normal force is

$$F_n=\frac{8}{3}\frac{\mu_g}{1-\nu_g}R\left(\frac{\xi}{R}\right)^{3/2},$$

where μ_g is the shear modulus and ν_g the Poisson ratio. If half the tangential separation between the sphere center is Δs, the tangential force is then

$$\Delta F_t=\frac{8\mu_g}{2-\nu_g}R\left(\frac{\xi}{R}\right)^{1/2}\Delta s.$$

Finally, one may obtain, from mean-field granular displacement, the elastic constant values, i.e., the bulk modulus

$$K_{\mathrm{MF}}=\frac{1}{3\pi}\frac{\mu_g}{(1-\nu_g)}(\Phi Z)^{2/3}\left(\frac{3\pi(1-\nu_g)}{2\mu_g}P\right)^{1/3}$$

and the shear modulus

$$\mu_{\mathrm{MF}}=\left(\frac{1}{1-\nu_g}+\varepsilon\frac{3}{2-\nu_g}\right)\frac{\mu_g}{5\pi}(\Phi Z)^{2/3}\left(\frac{3\pi(1-\nu_g)}{2\mu_g}P\right)^{1/3}$$

with two limits: (i) No sliding friction between the grains (take $\varepsilon=0$) or (ii) infinite friction between the grains (take $\varepsilon=1$). For the macroscopic Jiang-Liu model in the isotropic case, the strain and stress tensors read

$$u_{ij}=-\frac{\delta_0}{3}\delta_{ij},\quad \sigma_{ij}=P\delta_{ij},\quad P=E\mathcal{B}\delta_0^{3/2}. \tag{5}$$

For an isotropic compression, we have $P=E\mathcal{B}\delta_0^{3/2}=K_{\mathrm{MF}}\delta_0$; therefore

$$K_{\mathrm{MF}}\equiv E\mathcal{B}\left(\frac{P}{E\mathcal{B}}\right)^{1/3}.$$

Consequently,

$$\mathcal{B}=\frac{\Phi Z}{2^{3/2}3\pi(1-\nu_g^2)}. \tag{6}$$

C. Determination of the ratio $\mathcal{B}/\mathcal{A}$

1. Mean field

Now we consider the Jiang-Liu model with x-z shear under isotropic compression P:

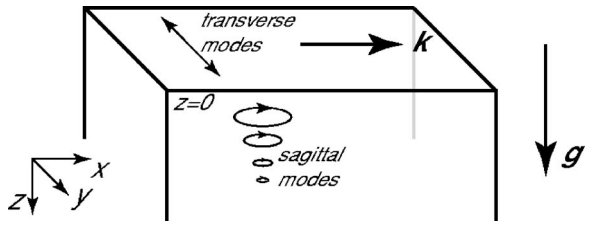

FIG. 2. Theoretical setup. We consider elastic waves propagating along the x direction in a cell filled with granular matter. Gravity is along the z axis. The y axis is the direction transverse to propagation.

$$\sigma_{xz}=-2\mathcal{A}E\delta_0^{1/2}=-2\mu_{\mathrm{MF}}u_{xz}$$

and $P=E\mathcal{B}\delta_0^{3/2}$, thus $\mu_{\mathrm{MF}}\equiv E\mathcal{A}(P/E\mathcal{B})^{1/3}$. Therefore,

$$\mathcal{A}=\frac{\Phi Z}{2^{3/2}5\pi(1+\nu_g)}\left(\frac{1}{1-\nu_g}+\frac{3\varepsilon}{2-\nu_g}\right). \tag{7}$$

If one takes $\Phi\simeq 0.6$ and $Z\simeq 6$. The bulk shear modulus for silica oxide is $\mu_g\simeq 30$ GPa and the Poisson ratio is $\nu_g\simeq 0.2$. This gives $E\mathcal{B}\simeq 10$ GPa and $E\mathcal{A}\simeq 6.5$ GPa for $\varepsilon=0$ and $E\mathcal{A}\simeq 9$ GPa for $\varepsilon=1$. These values will be of importance when the surface sound wave velocities, found experimentally for sand, will be discussed at the end of the paper. From the above expressions, we get

$$\frac{\mathcal{B}}{\mathcal{A}}=\frac{5}{3\left(1+\frac{3\varepsilon(1-\nu_g)}{2-\nu_g}\right)}. \tag{8}$$

For $\varepsilon=0$, we get $\mathcal{B}/\mathcal{A}=5/3$. For $\varepsilon=1$ and $\nu_g=0.2$, we get $\mathcal{B}/\mathcal{A}=5/7$.

2. Energetic argument

According to Jiang and Liu, we have a material instability corresponding to a Coulomb yield, for a criterion based on the free energy landscape convexity (a thermodynamic stability criterion) [34]:

$$\tan\theta=\sqrt{\frac{2\mathcal{A}}{\mathcal{B}}}. \tag{9}$$

Thus $\mathcal{B}/\mathcal{A}=2/\tan^2\theta_c\simeq 6$. We then notice a large discrepancy for the $\mathcal{B}/\mathcal{A}$ ratio between the mean-field solution and the empirical result obtained from direct measurement of the sand-pile slope.

III. SAGITTAL WAVES UNDER GRAVITY

A. Equilibrium of the system

Now we examine the case of a semi-infinite volume filled with granular matter and submitted to a vertical gravity field (Fig. 2). As mentioned in the Introduction, due to the inhomogeneous pressure field $P\propto\rho gz$, the system presents a stratification in the propagation speed $c\propto z^{1/6}$ which should also lead to a refraction toward the free surface. A simple qualitative picture, recently proposed by Gussev [33], establishes a relation between the wave propagation confined

within an effective waveguide and vertical resonances due to multiple reflections of the curved propagation rays at the upper free surface. This vision is somehow opposed to the early claim of Liu and Nagel [4] that the free surface would absorb the wave: The reflection is actually total.

The first step is to compute the reference state of the system. We first solve the equilibrium problem, starting from a strain tensor of the form

$$u_{ij} = \begin{pmatrix} 0 & 0 & 0 \\ 0 & 0 & 0 \\ 0 & 0 & -\delta_0 \end{pmatrix}, \quad u_{ij}^0 = \delta_0 \begin{pmatrix} \frac{1}{3} & 0 & 0 \\ 0 & \frac{1}{3} & 0 \\ 0 & 0 & -\frac{2}{3} \end{pmatrix}.$$

The modulus follows as $u_s^2 = (2/3)\delta_0^2$. Using the constitutive relation, we obtain the stress tensor

$$\sigma_{ij} = E\delta_0^{3/2} \begin{pmatrix} \left(\mathcal{B} - \frac{\mathcal{A}}{3}\right) & 0 & 0 \\ 0 & \left(\mathcal{B} - \frac{\mathcal{A}}{3}\right) & 0 \\ 0 & 0 & \left(\mathcal{B} + \frac{5\mathcal{A}}{3}\right) \end{pmatrix}.$$

The pressure is defined from the trace of this stress tensor: $P = E\delta_0^{3/2}(\mathcal{B} + \mathcal{A}/3)$. The expression for the vertical stress is replaced by

$$\sigma_{zz} = \left(\mathcal{B} + \frac{5\mathcal{A}}{3}\right) E\delta_0^{3/2} = \rho g z$$

so that the volumic compression reads

$$\delta_0 = -\frac{dW_0}{dz} = \left(\frac{\rho g z}{E\left(\mathcal{B} + \frac{5\mathcal{A}}{3}\right)}\right)^{2/3}, \tag{10}$$

where W_0 is the vertical displacement field. The second boundary condition is taken at $z \to \infty$. In practice, we impose a null displacement $W_0(H) = 0$ at the lower edge of a box $z = H$ and at the end let H tend to infinity (see Appendixes B and C for details about finite depth effects).

B. Linearized equations

Now we investigate the existence of propagative modes polarized in the sagittal plane (x, z). We consider the deformation of the free surface to be of the form $\zeta(x,t) = \zeta_0 e^{i(kx - \omega t)}$. The displacement field is defined through two dimensionless functions U and W of the dimensionless variable $\eta = kz$:

$$\tilde{\mathbf{U}} = \begin{pmatrix} iU(\eta) \\ 0 \\ W(\eta) \end{pmatrix} \zeta.$$

The disturbance to the strain tensor reads

$$\widetilde{u_{ij}} = k\zeta \begin{pmatrix} -U & 0 & \frac{i(U' + W)}{2} \\ 0 & 0 & 0 \\ \frac{i(U' + W)}{2} & 0 & W' \end{pmatrix}$$

and its traceless counterpart is

$$\widetilde{u_{ij}}^0 = k\zeta \begin{pmatrix} -\frac{2U}{3} - \frac{W'}{3} & 0 & \frac{i(U' + W)}{2} \\ 0 & \frac{U}{3} - \frac{W'}{3} & 0 \\ \frac{i(U' + W)}{2} & 0 & \frac{2W'}{3} + \frac{U}{3} \end{pmatrix}.$$

The disturbance to the volumic compression is $\tilde{\delta} = k\zeta(U - W')$. That of the modulus u_s^2 reads

$$\widetilde{u_s^2} = 2u_{ij}^0 \widetilde{u_{ij}^0} = -\frac{2\delta_0}{3}(U + 2W')k\zeta.$$

The disturbance to the stress tensor may be formally expressed as

$$\tilde{\sigma}_{ij} = \sqrt{\delta_0} E \left[\frac{3}{2}\mathcal{B}\tilde{\delta}\delta_{ij} - \mathcal{A} \begin{pmatrix} \frac{1}{3} & 0 & 0 \\ 0 & \frac{1}{3} & 0 \\ 0 & 0 & -\frac{2}{3} \end{pmatrix} \tilde{\delta} - 2\mathcal{A}\widetilde{u_{ij}}^0 - \frac{\mathcal{A}}{6}\tilde{\delta}\delta_{ij} + \frac{\mathcal{A}}{2\delta_0}\widetilde{u_s^2}\delta_{ij} \right]$$

which gives, after simplification, the following expressions for its components:

$$\widetilde{\sigma_{xx}} = E\sqrt{\delta_0}\left[\left(\frac{\mathcal{A}}{2} + \frac{3\mathcal{B}}{2}\right)U + \left(\frac{\mathcal{A}}{2} - \frac{3\mathcal{B}}{2}\right)W'\right]k\zeta,$$

$$\widetilde{\sigma_{zz}} = -E\sqrt{\delta_0}\left[\left(\frac{\mathcal{A}}{2} - \frac{3\mathcal{B}}{2}\right)U + \left(\frac{5\mathcal{A}}{2} + \frac{3\mathcal{B}}{2}\right)W'\right]k\zeta,$$

$$\widetilde{\sigma_{xz}} = \widetilde{\sigma_{zx}} = -i\mathcal{A}E\sqrt{\delta_0}(U' + W)k\zeta.$$

For the sake of simplicity, we rescale the stress tensor, introducing the functions $S_{xz}(kz)$, $S_{zz}(kz)$, and $S_{xx}(kz)$:

$$\widetilde{\sigma_{xz}} = i\rho\Gamma^2 k^{2/3}\zeta S_{xz}(kz),$$

$$\widetilde{\sigma_{zz}} = \rho\Gamma^2 k^{2/3}\zeta S_{zz}(kz),$$

$$\widetilde{\sigma_{xx}} = \rho\Gamma^2 k^{2/3}\zeta S_{xx}(kz), \tag{11}$$

where Γ is a material parameter of dimension $[T^{-1}L^{5/6}]$ defined by

$$\Gamma = \mathcal{A}^{1/2}(\mathcal{B} + 5\mathcal{A}/3)^{-1/6}\left(\frac{E}{\rho}\right)^{1/3} g^{1/6}. \tag{12}$$

The previous expressions then simplify into

$$S_{xx}(\eta) = \eta^{1/3}\left[\left(\frac{1}{2} + \frac{3\mathcal{B}}{2\mathcal{A}}\right)U(\eta) + \left(\frac{1}{2} - \frac{3\mathcal{B}}{2\mathcal{A}}\right)W'(\eta)\right],$$

$$S_{zz}(\eta) = -\eta^{1/3}\left[\left(\frac{1}{2} - \frac{3\mathcal{B}}{2\mathcal{A}}\right)U(\eta) + \left(\frac{5}{2} + \frac{3\mathcal{B}}{2\mathcal{A}}\right)W'(\eta)\right],$$

$$S_{xz}(\eta) = -\eta^{1/3}[U'(\eta) + W(\eta)]. \tag{13}$$

From the equations of motion, we get the dispersion relationship

$$\omega = \alpha\Gamma k^{5/6}. \tag{14}$$

The dimensionless set of equations

$$\alpha^2 U = S_{xx} + S'_{xz}, \tag{15}$$

$$\alpha^2 W = -S_{xz} + S'_{zz} \tag{16}$$

determines the shape of the modes and, through the boundary conditions, fixes the dimensionless frequency α. We can already conclude that surface modes do exist and are (weakly) dispersive. Indeed, the group velocity increases as $k^{1/6}$ or equivalently as $\omega^{1/5}$.

C. Resolution

Now, in order to obtain the prefactor α of the dispersion relation (14) as well as the shape of the modes, we solve the boundary condition problem, rewriting the above equations as a set of 4—linear—ordinary differential equations:

$$U' = -W - \eta^{-1/3}S_{xz},$$

$$W' = -\frac{1}{5\mathcal{A} + 3\mathcal{B}}[(\mathcal{A} - 3\mathcal{B})U + 2\mathcal{A}\eta^{-1/3}S_{zz}],$$

$$S'_{xz} = \alpha^2 U - S_{xx},$$

$$S'_{zz} = \alpha^2 W + S_{xz},$$

$$S_{xx} = \frac{1}{5\mathcal{A} + 3\mathcal{B}}[(3\mathcal{B} - \mathcal{A})S_{zz} + 2(\mathcal{A} + 6\mathcal{B})\eta^{1/3}U].$$

The boundary conditions are vanishing stresses $S_{xz}(0)=0$ and $S_{zz}(0)=0$ at the surface and a vanishing strain at infinity:

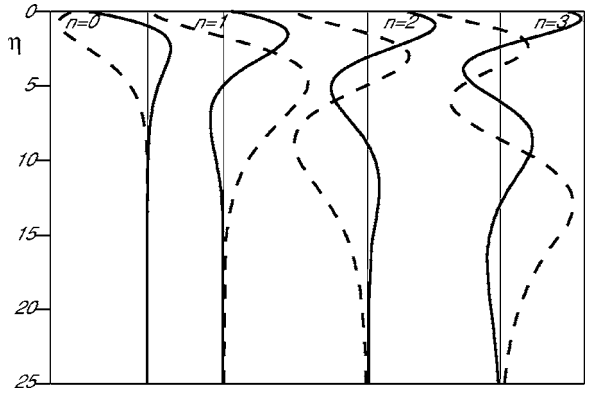

FIG. 3. Shape of the sagittal modes: Profiles of the horizontal displacement $U(\eta)$ (solid line) and vertical displacement $W(\eta)$ (dashed line). $\eta=kz$ is the reduced depth.

$U(\eta\to\infty)=0$ and $W(\eta\to\infty)=0$. This selects unique asymptotic behaviors. Note in particular that S_{xz} and S_{zz} vanish linearly with η so that $\eta^{-1/3}S_{xz}$ and $\eta^{-1/3}S_{zz}$ are well-behaved terms. The same condition is obtained if one starts with a finite load at the surface (so that the elastic moduli do not vanish anymore) and lets this extra load tend to zero.

The amplitude is normalized using $W(0)=1$. The solution $[U, W, S_{xz}, S_{zz}](\eta)$ is obtained by superposition of the solutions obtained, starting from the initial conditions [0, 1, 0, 0] and [1, 0, 0, 0]. In practice, we tune the value of α to get the cancellation of both U and W at a finite depth H, and then take the limit $H\to\infty$ (see Appendix C for the discussion of finite depth H effects).

Hence the sagittal surface waves present a discrete number of modes guided by the refractive index grading induced by gravity. The shape of the modes excited at a given pulsation ω is displayed on Fig. 3. They are elliptically polarized, the principal axis being along x and z. The modes are essentially localized in surface, on a depth of order $(n+1)$ times the wavelength $\lambda=2\pi/k$. The dispersion relationship is displayed on Fig. 4 for a particular value of Γ. One observes that the different branches are pretty close to each other. This

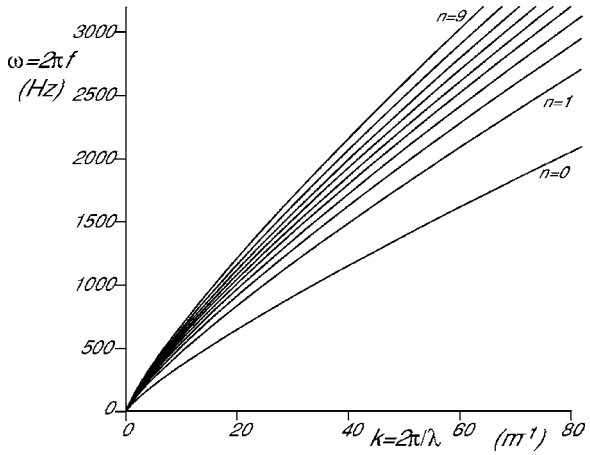

FIG. 4. Dispersion relation of sagittal waves for $\Gamma = 50\ \mathrm{s}^{-1}\ \mathrm{m}^{5/6}$. Note that the dispersion relation of transverse waves (not shown) almost collapses on the same curves.

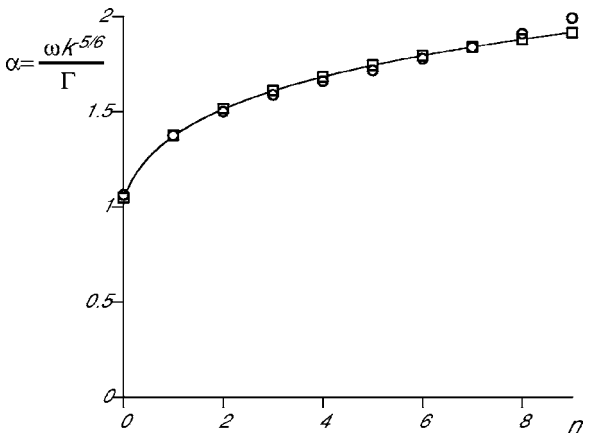

FIG. 5. Dimensionless frequency $\alpha=\omega k^{-5/6}/\Gamma$ as a function of the mode number n for the longitudinal (○) and the transverse (□) modes. The best fit (solid line) of transverse modes data by $\alpha=(\alpha_0+\delta_\alpha n)^{1/6}$ gives $\alpha_0\simeq 1.3906$ and $\delta_\alpha\simeq 5.4145$.

is due to the very slow increase of the dimensionless frequency α with the mode number n (Fig. 5). Although the values of α are not regularly spaced, they follow a general trend: $\alpha\sim n^{1/6}$.

IV. TRANSVERSE SURFACE WAVES UNDER GRAVITY

A. Linearized equations

Now we investigate the existence of propagative transverse modes localized close to the surface [36]. We consider a transverse displacement $\zeta(x,t)=\zeta_0 e^{i(kx-\omega t)}$ at the surface of the granular bed. We define the dimensionless function V of the dimensionless variable $\eta=kz$:

$$\tilde{\mathbf{U}}=\begin{pmatrix}0\\ V(\eta)\\ 0\end{pmatrix}\zeta. \tag{17}$$

Again, we linearize the strain tensor

$$\widetilde{u_{ij}}=k\zeta\begin{pmatrix}0 & \frac{iV}{2} & 0\\ \frac{iV}{2} & 0 & \frac{V'}{2}\\ 0 & \frac{V'}{2} & 0\end{pmatrix}$$

and find no variation of the volumic compression $\tilde{\delta}=0$. The trace of $\widetilde{u_{ij}}$ is null so that $\widetilde{u_{ij}}^0=\widetilde{u_{ij}}$, and then $\widetilde{u_s}^2=2u_{ij}u_{ij}$ vanishes. Finally, we obtain

$$\tilde{\sigma}_{ij}=-2\mathcal{A}E\sqrt{\delta_0}\widetilde{u_{ij}}=-\mathcal{A}E\sqrt{\delta_0}k\zeta\begin{pmatrix}0 & iV & 0\\ iV & 0 & V'\\ 0 & V' & 0\end{pmatrix}.$$

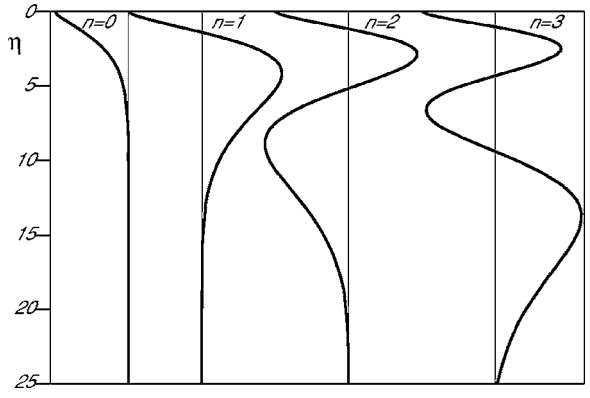

FIG. 6. Shape of the transverse modes $V(\eta)$ for the same frequency.

From the equation of motion along y, we get a similar dispersion relation as for sagittal modes:

$$\omega=\alpha\Gamma k^{5/6}. \tag{18}$$

The shape of the mode—and the α values—are now given by the equation

$$\alpha^2 V=\eta^{1/3}V-(\eta^{1/3}V'). \tag{19}$$

B. Resolution

To solve Eq. (19), we decompose the problem in two equations:

$$V'=\eta^{-1/3}S,$$

$$S'=(\eta^{1/3}-\alpha^2)V,$$

with boundary conditions coming from the zero stress condition at the free surface $[S(0)=0]$ and the definition of ζ $[V(0)=1]$. At infinity, we impose a vanishing displacement: $V(\eta\to\infty)=0$. As for sagittal waves, the system presents a discrete number of modes that may be associated with the gravity induced stratification. The shape of the modes is displayed on Fig. 6. The motion is pure shear and the modes are linearly polarized in the direction transverse to the sagittal plane. The amplitude of the mode n decays exponentially after typically n oscillations. Figure 5 shows the variation of the dimensionless frequency α with n. Numerically obtained data are well fitted by $\alpha=(\alpha_0^6+\delta_\alpha n)^{1/6}$, with $\alpha_0\simeq 1.07$ and $\delta_\alpha\simeq 5.35$.

V. THE SONG OF DUNES: SURFACE WAVES INDUCED BY AN AVALANCHE

A. Dispersion relation in a booming sand

In the Introduction, we summarized the state of the art concerning the song of dunes. Now that we have clarified theoretically the nature of surface elastic waves, it is interesting to investigate whether or not field (and other) measurements can be matched using this concept. In a previous article, Andreotti [19] has measured the dispersion relation at

the surface of the avalanche slip face of a singing dune (top schematic of Fig. 7). Now we briefly recall the measurement methodology but extensive details can be found in this last reference. Sinusoidal signals, recorded on a tape, were played through an amplified loudspeaker that was kept fixed. As the mechanical transmission of the sound generator with the sand bed is nonlinear, the signal is distorted and presents harmonics. This imperfection was used to derive several points of the dispersion relation from each recording. From the phase between the Fourier components of the signals of two accelerometers aligned with the loudspeaker, the wavelengths λ associated with each frequency f were obtained. In order to unwrap the phase, the amplitude of the signals was slightly modulated at low frequency. The collection of all measurements that establishes the dispersion relation is presented in Fig. 7.

Once replaced in the context of surface elastic waves, the wide scatter of experimental data points is not completely surprising. Indeed, a localized excitation at the surface, such as the one used for these measurements, cannot select a single mode. It is even probable that the decomposition of the source into sagittal and transverse modes may vary from one realization to the other. Thus the measured phase just gives an effective wavelength. To reanalyze the data, we considered that the lower frequency for a given wavelength was a pure mode $n=0$. The best fit of this lower bound by the relation $\omega=\alpha_0\Gamma k^{5/6}$ yields a value $\Gamma\simeq 50\ \mathrm{s}^{-1}\ \mathrm{m}^{5/6}$. It would correspond at the booming emission frequency $f=100$ Hz to a phase velocity of 32 m/s and to a group velocity of 27 m/s for the mode $n=0$. But, of course, higher order modes can propagate much faster than this lower bound.

Clearly, Fig. 7 does not constitute a proof that the propagation of surface waves is well captured by the model and more controlled experiments are needed to confirm our analysis. Nevertheless, as can be evidenced on the figure, the agreement for the first three modes is not bad and it is interesting now to compare the value found for Γ to the one predicted by a mean-field estimate. For $EB=10$ GPa and the ratio $\mathcal{B}/\mathcal{A}=6$ derived from the sand-pile slope, we obtain $\Gamma\simeq 106\ \mathrm{s}^{-1}\ \mathrm{m}^{5/6}$. It means that the actual surface wave speeds measured in these conditions are still slow by a factor of 2 when evaluated from the simple arguments presented above. While the mean-field evaluation of the compression modulus EB is in general good, it usually overestimates the shear modulus [29]. Here, it suggests that the ratio $\mathcal{B}/\mathcal{A}$ is in fact around 29 instead of 6 as argued by Liu *et al.* [34] from a Coulomb yield argument based on a sand pile slope.

B. Finite size effect

In a semi-infinite medium, we have seen that the surface elastic waves always exist. If we now consider that the displacement should vanish at a finite depth H, a waveguide cutoff frequency appears, below which no sound can propagate (see the Appendixes). It corresponds to the limit of vanishing kH and thus to a nonpropagative mode. In Appendices B and C, the shape of these resonant modes has been derived analytically as well as a good approximation for the resonance frequencies. We will limit ourselves to discussion of the results, presented in Fig. 8, in the context of booming avalanches, where they turn out to be useful.

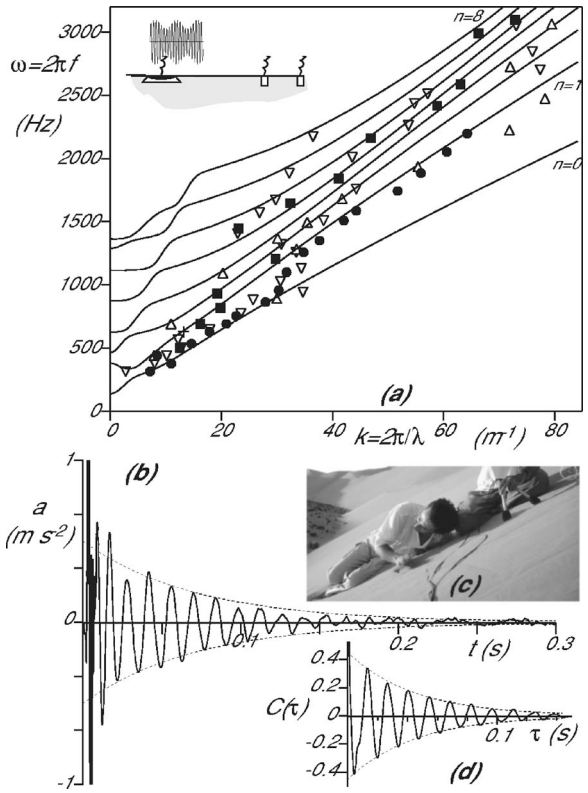

FIG. 7. (a) Dispersion relation of surface elastic waves on the slip face of a booming dune. A sinusoidal signal is emitted by a loudspeaker, aligned with transducers distant by 5 cm (▽), 15 cm (△), 25 cm (■), and 42 cm (●). The solid lines correspond to the sagittal Rayleigh-Hertz modes [see Eq. (14) and the Appendix C] with a material stiffness $\Gamma\simeq 50\ \mathrm{s}^{-1}\ \mathrm{m}^{5/6}$ adjusted to match the lowest $n=0$ propagating mode. The cutoff frequency is determined independently [(b)–(d)]. (b) Response of the booming dune to a normal tap, at the same place as (a). The signal is similar when recorded in the sand bed with an accelerometer or in the air with a microphone. The tail following the tap contains a well defined frequency, interpreted here as the first compression resonant mode due to the presence of wet sand at a depth around 50 cm below the surface. (c) Photograph showing the Makhnovist drum experiment. (d) Autocorrelation function of the signal shown in (b). The resonant frequency is around 73 Hz for the conditions of the experiment.

Also they apparently resemble sinusoidal modes, there is a strong difference with usual modes in a nondispersive homogeneous medium: The resonant frequency f is proportional to $\Gamma H^{-5/6}$. Thus the nondispersive relation invoked in [20,21] does not apply since there is not a single sound velocity but a discrete number of dispersive modes.

Also, surprisingly, it is a well known fact that the desert dunes are filled with this water trapped by capillarity. Moreover, due to the successive avalanches, there is a layering of wet and dry zones close to the surface finishing at the surface with a dry layer (see schematic on Fig. 1). In the singing megabarchan located close to Sidi-Aghfinir (Morocco), we

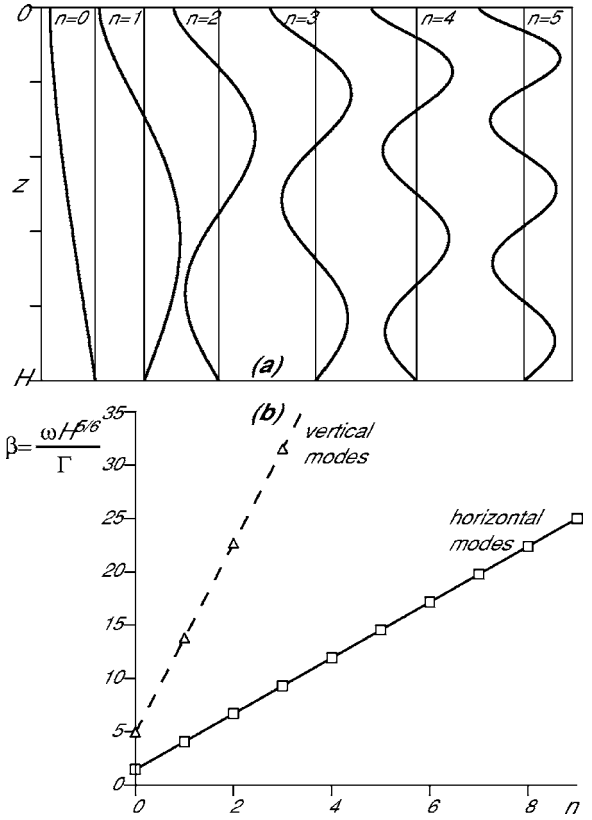

FIG. 8. (a) Shape of the resonant—not propagative—modes. (b) Rescaled resonant frequencies β of vertical ($\triangle$) and horizontal ($\square$) modes, together with the analytical approximation given in Appendix B.

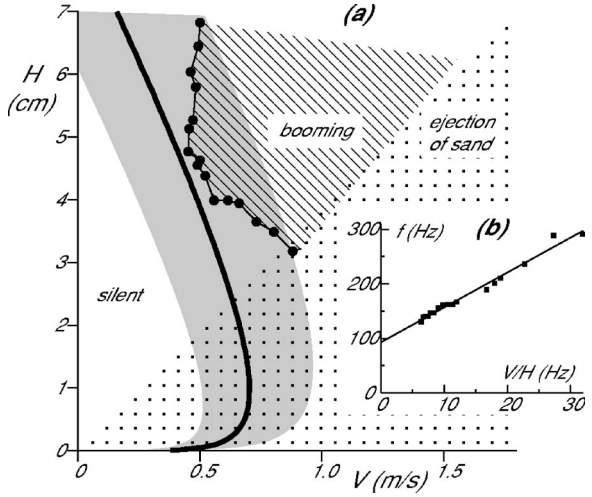

FIG. 9. Parameter range for sound emission in the Douady *et al.* laboratory experiment (Fig. 3 of [21]), depending on the pushing velocity V and the height of pushed sand H. The symbols ($\bigcirc$) are the experimental data. The dashed zone is the region of parameters for which there is spontaneous emission of sound and the dotted zone is that for which sand is ejected. The line shows the predicted limit on the left of which surface waves cannot propagate due to waveguide cutoff (see text for details). As there are important sources of error (for instance on Γ), we have represented the error bars by a gray zone. However, the solid line prediction was obtained without any adjustable parameter. Γ is determined on the same sand coming from the Atlantic Sahara (Fig. 7). (b) The emission frequency f is taken from a subset of data in Douady *et al.* close to the instability threshold and plotted as a function of V/H. The relation is well fitted by $f=0.38\sqrt{g/d}+6.4V/H$.

have observed that the first dry layer is at a depth H ranging from a few centimeters to one meter. Figure 7(b) shows the response to a tap given with the hand on the surface of the dune [the so-called Makhnovist drum experiment shown on Fig. 7(c)]. As for the song of dunes itself, measurements of the pressure signal in the air and of the surface acceleration signal are very similar. While the impact is very short, the response is quite long, with well defined oscillations that decrease exponentially. The systematic study of this resonance remains to be done in a systematic way. Still, after preliminary studies in the lab, we think that it is related to a finite depth effect. The resonant frequency was derived from the first maximum of the signal autocorrelation function [Fig. 7(d)]. It gives $f=73$ Hz which is well below the spontaneous frequency of emission ($\simeq 100$ Hz). This resonant frequency corresponds in our theory to $H=47$ cm, which is indeed the typical depth at which the first wet layer may be found on dry days. The Q factor of the resonator, defined as the angular frequency times the relaxation time, is around 33. The solid lines in Fig. 7(a) actually correspond to the dispersion relation, computed with a null displacement imposed at a depth H (see Appendix C).

It is not completely obvious that the wet zone inside the dune plays the role of a rigid boundary. Indeed, the porous medium constituted by the grains is not saturated in water (which would create a strong impedance mismatch): The sand becomes cohesive due to the formation of capillary bridges between the grains. As a consequence, the normal force exerted on grains and thus the sound velocity increases. Since the capillary pressure is proportional to the surface tension γ divided by the grain diameter d, it is only a few times the pressure induced by gravity at 10 cm below the surface. Due to the small exponent of the sound speed–pressure relation, the sound velocity should not vary much at the interface between dry and wet sand (typically 10% at 50 cm below the surface). However, the second effect of capillary bridges is to increase the dissipation of energy by viscous damping inside water. The most dissipative zone is probably inside the grains contact area. Using common estimates of the microcontacts geometry, we find a relaxation time in the presence of water of the order of $\simeq 1$ ms, which is consistent with the measurements performed at high frequency by [37]. This is two orders of magnitude smaller than the relaxation time measured for a dry sand layer (Fig. 9). As a conclusion, the wet layer probably acts as an efficient acoustic absorber. Although not completely equivalent, it should act as a rigid boundary, cutting the low frequency modes that would otherwise be propagating in a dry sand.

C. The booming instability threshold

The previous study suggests an alternative explanation for the booming instability threshold reported in [21], i.e., dunes

cannot boom if the first dry layer is too close to the surface, as surface elastic waves cannot propagate. For an emission at $f=100$ Hz, the predicted minimum depth H is around 7.5 cm—by comparison, typical booming avalanches are 2 cm to 5 cm thick (Fig. 1). Even under some circumstances, we have observed that too thin flowing layers do not boom, as reported in [21]. The booming instability threshold was measured by [21] in a controlled experiment (see Introduction), where the height H and the velocity V of a small scale avalanche were controlled. Note, however, that H corresponds to a typical vertical scale but the geometry of the whole avalanching apparatus is more complicated. The experiment shows that the emission frequency f and the threshold depend on V and H in a complex manner (Fig. 9). We have plotted on the same graph the curve on the left of which surface elastic waves cannot propagate due to the finite depth cutoff. The elastic wave parameters were taken from the previously discussed measurement on naturally booming dunes (with the same sand). The emission frequency f close to the threshold is fitted from the experimental points of Douady *et al.* [21] by a linear relation on V/H [Fig. 9(b)]. The effective depth of the resonator was taken equal to the avalanche height H. We see that the predicted threshold goes close enough to the experimental points, without any adjustable parameter. Of course, it would be nice to refine the calculation, taking into account the complexity of the experimental setup geometry, but this is out of the scope of the present paper. We clearly see here that booming is heard whenever surface elastic waves are able to propagate, given the overall sand depth. As a conclusion, the correct assessment of surface waves dispersion shows that there is no need to introduce "coupling (shear?) waves" propagating at the very small velocity of 1 m/s in order to explain the booming threshold. This is in agreement with what was previously reported in this context by [19].

D. The song of dunes as a coupling between avalanching grains and surface elastic waves

To conclude this section, the theoretical investigation of elastic waves at the surface of a granular bed sheds light on the mechanisms at work in the song of dunes. These waves have been evidenced in the field [19] and their existence is now proven in the context of nonlinear elasticity. The comparison of the theory with the measured dispersion relation has allowed us to deduce the material parameter Γ, which is (only) a factor of 2 below the mean field prediction. Using this value, the threshold above which surface waves at the emission frequency (governed by the shear rate) can propagate is determined and matches quantitatively the threshold measured by [21].

These results allow us to clarify the role of resonance for the booming dune instability. For a given resonator height, the experiment allows us to increase the collision frequency in the shear zone (by increasing the velocity) up to the cutoff frequency (resonance condition). But the instability is still present for a collision rate (i.e., an emission frequency) larger than the cutoff frequency. In this case, the excited elastic modes are propagative and the sand booming frequency, selected by the shear rate, is no longer a resonant condition.

Still, several problems raised by the song of dunes remain open. (i) The exact location in avalanches of the shear band exciting waves is still unclear. Can one produce a controlled sounding avalanche in which the velocity profile and the emission frequency can be simultaneously measured? (ii) Can one prove the direct relation between the resonant frequency (obtained for instance by tapping) and the emission threshold? (iii) It has been shown that singing grains are covered by a specific silica-gel layer [18], which may dry the contact between grains and thus decrease the wave damping. We have shown here that the Q factor of a resonator constituted by sounding grains can be of the order of 33, which is impressively high. Can one prove, by studying the propagation of surface waves in the lab, that there is a difference (propagation speed or attenuation rate) between silent and sounding grains?

VI. CONCLUSION

In conclusion, we have performed a derivation of sound-wave propagation modes in the context of the Jiang-Liu model of granular nonlinear elasticity. Under gravity, we prove the existence of a discrete number of modes localized in the vicinity of the free surface. They are due to a stratification of the material stiffness, responsible for a channeling effect of the acoustic waves. The waves can be either elliptically polarized in the sagittal plane or linearly polarized in the transverse direction. It is interesting to note that the polarization becomes linear if the shear modulus vanishes ($\mathcal{A}=0$) [33]. The identified modes are dispersive, which means that there is not one single propagation speed c characteristic of the material: There is a multiplicity of modes very close to each other; each mode follows a dispersion relation of the type $\omega \propto \Gamma k^{5/6}$.

Note additionally that all the results presented here are very robust to slight changes in the model. For instance, we have shown that imposing the boundary condition at finite depth only leads to a waveguide effect, with a cutoff frequency given by the resonant modes (see the Appendixes). We have also checked explicitly that a load at the free surface (a nonvanishing pressure) does not change the number nor the nature of the modes. In particular, no supplementary mode corresponding to the usual Rayleigh wave appears: The sagittal modes replace Rayleigh ones. For this reason, we propose to call "Rayleigh-Hertz modes" the modes identified in this paper. We also checked that the same modes are also present in the Boussinesq approximation [35].

We have mostly discussed the theoretical findings in the context of booming avalanches, which initially motivated the present work. The semiquantitative agreement about the dispersion relation and the instability threshold are encouraging, and confirms the mechanism of interaction between surface waves and avalanching grains proposed a few years ago [19]. The next step is to prove experimentally the existence of surface waves and resonant modes and to investigate where they can be described by nonlinear elasticity. This is an ongoing work in our laboratory and we leave these questions for a future paper.

ACKNOWLEDGMENTS

We wish to thank P. Claudin for fruitful discussion on the effective strain-stress relation in granular matter and V. Goussev, who worked independently on the same subject, for long and pleasant discussions on the nature of these waves (guided vs Rayleigh). B.A. thanks H. Elbelrhiti and H. Bellot for assistance during the first field measurements. This study was supported by an "ACI Jeunes Chercheurs" of the French ministry of research.

APPENDIX A: SOUND PROPAGATION UNDER ISOTROPIC COMPRESSION

1. Propagation speed of longitudinal waves under isotropic compression

For the sake of completeness, we derive here the expressions of the propagation speed under isotropic compression. This can be useful to determine the parameters of the model from preliminary experiments under load. We consider first the propagation of longitudinal waves along the x axis. As the system is homogeneous, the modes are simply Fourier modes of the form $Ue^{i(kx-\omega t)}$. We denote by $\widetilde{u_{ij}}$ the disturbance to the strain field and $\widetilde{u_{ij}}^0$ its traceless counterpart:

$$\widetilde{u_{ij}} = ikU\begin{pmatrix} 1 & 0 & 0 \\ 0 & 0 & 0 \\ 0 & 0 & 0 \end{pmatrix}, \quad \widetilde{u_{ij}}^0 = ikU\begin{pmatrix} \frac{2}{3} & 0 & 0 \\ 0 & -\frac{1}{3} & 0 \\ 0 & 0 & -\frac{1}{3} \end{pmatrix}.$$

The disturbance of the volumic compression is then $\tilde{\delta} = -ikU$ and that of the modulus u_s^2 is null. The stress associated with the sound wave is

$$\widetilde{\sigma_{ij}} = E\sqrt{\delta_0}\left[\frac{3}{2}\mathcal{B}\tilde{\delta}\delta_{ij} - 2\mathcal{A}\widetilde{u_{ij}}^0\right],$$

so that the equation of motion finally reads

$$-\rho\omega^2 U = -k^2 E\sqrt{\delta_0}\left[\frac{3}{2}\mathcal{B} + \frac{4}{3}\mathcal{A}\right]U. \tag{A1}$$

The speed of longitudinal acoustic waves is finally

$$c = \gamma_{\parallel}\left(\frac{P}{E}\right)^{1/6}\sqrt{\frac{E}{\rho}}, \tag{A2}$$

with $\gamma_{\parallel} = [(3/2)\mathcal{B} + (4/3)\mathcal{A}]^{1/2}\mathcal{B}^{-1/6}$. We thus recover the scaling of the speed of sound c as $P^{1/6}$, but with an extra dependence on the coefficients $\mathcal{A}$ and $\mathcal{B}$ which themselves depend on the mean number of contacts and thus on pressure.

2. Propagation speed of transverse waves under isotropic compression

Similarly, we consider the propagation of transverse waves along the x axis. The modes are still Fourier modes of the form $Ve^{i(kx-\omega t)}$,

$$\widetilde{u_{ij}} = ikV\begin{pmatrix} 0 & 1/2 & 0 \\ 1/2 & 0 & 0 \\ 0 & 0 & 0 \end{pmatrix}.$$

The disturbance of the volumic compression $\tilde{\delta}$ and of the modulus u_s^2 are both null. The disturbance to the stress reduces to

$$\widetilde{\sigma_{ij}} = -2E\sqrt{\delta_0}\mathcal{A}\widetilde{u_{ij}}^0$$

and the equation of motion finally reads

$$-\rho\omega^2 V = -k^2 E\sqrt{\delta_0}\mathcal{A}V. \tag{A3}$$

The speed of longitudinal acoustic waves is finally

$$c = \gamma_{\perp}\left(\frac{P}{E}\right)^{1/6}\sqrt{\frac{E}{\rho}}, \tag{A4}$$

with $\gamma_{\perp} = \mathcal{A}^{1/2}\mathcal{B}^{-1/6}$.

We thus get a prediction for the relation between the propagation speeds of longitudinal and transverse waves: $\gamma_{\parallel}/\gamma_{\perp} = (3\mathcal{B}/2\mathcal{A} + 4/3)^{1/2} = (3/2\mu^2 - 7/6)^{1/2}$.

APPENDIX B: RESONANCES IN A FINITE DEPTH BOX

1. Horizontally polarized resonant modes

We consider the case of a granular packing bounded at $z=H$ by a rough bottom wall where the displacement vanishes. The semi-infinite case discussed at length in the body of the article corresponds to the limit where H tends to infinity. As H is the only relevant length scale of the problem, we now use the rescaled coordinate $\eta = z/H$. We consider nonpropagative modes of vibration whose disturbed displacement field is horizontal and of the form $U(\eta)e^{i\omega t}$. The disturbed strain field reads

$$\widetilde{u_{ij}} = \begin{pmatrix} 0 & 0 & U'(\eta)/2H \\ 0 & 0 & 0 \\ U'(\eta)/2H & 0 & 0 \end{pmatrix}.$$

The trace of $\widetilde{u_{ij}}$ is null so that $\tilde{\delta} = 0$, $\widetilde{u_{ij}}^0 = \widetilde{u_{ij}}$, and $\widetilde{u_s^2} = 2u_{ij}\widetilde{u_{ij}}$ vanishes. We end with $\tilde{\sigma}_{ij} = -2\mathcal{A}E\sqrt{\delta_0}\widetilde{u_{ij}}$. The disturbed vertical stress deduces as

$$\widetilde{\sigma_{zx}} = -\mathcal{A}E\sqrt{\delta_0}U'/H$$

and leads to the equation of motion

$$[\eta^{1/3}U'(\eta)]' + \beta^2 U(\eta) = 0, \tag{B1}$$

where β is the rescaled pulsation defined by

$$\omega = \beta\Gamma H^{-5/6}. \tag{B2}$$

Remarkably, the resonant frequencies are found to scale as $H^{-5/6}$ and not H^{-1} as for a nondispersive medium. A normalization condition can be added, for instance $U(0)=1$.

The solution of the ordinary equation (B1) involves the Bessel function of the first kind $J_{-2/5}$ and is of the form

$$U(\eta) = (3/5)^{2/5}\Gamma(3/5)\,\eta^{1/3}J_{-2/5}\left(\frac{6\beta}{5}\eta^{5/6}\right). \tag{B3}$$

For large η, U goes like $\eta^{-5/12}\cos((6\beta/5)\eta^{5/6}-\pi/20)$. The value of β is selected by the zero displacement condition at the bottom edge of the box, $U(1)=0$, which simplifies into $J_{-2/5}(6\beta/5)=0$. There is thus a discrete number of modes, labeled by n, whose rescaled frequency can be approximated by

$$\beta \simeq \frac{5\pi}{6}\left(n+\frac{11}{20}\right). \tag{B4}$$

The numerical evaluation of the rescaled resonant frequency β is plotted on Fig. 11 together with the analytical approximation. The agreement is almost perfect.

2. Vertically polarized resonant modes

We now consider modes of vibration whose disturbed displacement field is vertical and of the form $W(\eta)e^{i\omega t}$. Then the disturbed strain field reads

$$\widetilde{u_{ij}} = \begin{pmatrix} 0 & 0 & 0 \\ 0 & 0 & 0 \\ 0 & 0 & W'(\eta)/H \end{pmatrix}, \quad \widetilde{u_{ij}}^0 = \begin{pmatrix} -\frac{W'}{3H} & 0 & 0 \\ 0 & -\frac{W'}{3H} & 0 \\ 0 & 0 & \frac{2W'}{3H} \end{pmatrix}$$

from which we deduce the disturbed volumic compression $\tilde{\delta}=-W'/H$ and the disturbed modulus

$$\widetilde{u_s^2} = 2u_{ij}^0\widetilde{u_{ij}^0} = -\frac{4\delta_0 W'}{3H}.$$

Then the disturbed vertical stress is deduced as

$$\widetilde{\sigma_{zz}} = -\frac{E\sqrt{\delta_0}}{2H}(5\mathcal{A}+3\mathcal{B})W'.$$

It leads to an equation of motion similar to the previous one,

$$\left(\frac{5}{2}+\frac{3\mathcal{B}}{2\mathcal{A}}\right)[\eta^{1/3}W'(\eta)]' + \beta^2 W(\eta) = 0, \tag{B5}$$

and thus with the same type of solution. The rescaled resonant frequency β can now be approximated by

$$\beta = \frac{5\pi}{6}\left(\frac{5}{2}+\frac{3\mathcal{B}}{2\mathcal{A}}\right)^{1/2}\left(n+\frac{11}{20}\right). \tag{B6}$$

The numerical evaluation of the rescaled resonant frequency β is plotted on Fig. 11 for $\mathcal{B}/\mathcal{A}=6$ together with the analytical approximation. Again, the agreement is very good.

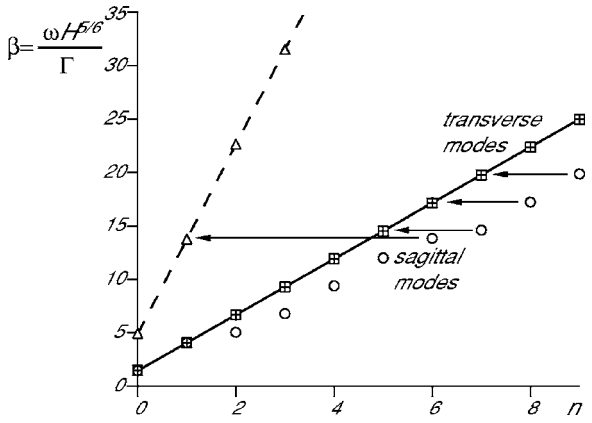

FIG. 11. Rescaled cutoff frequency β (i.e., rescaled frequency in the limit of small kH) as a function of the mode number for sagittal (○) and transverse (+) modes. The resonant frequencies of vertical (△) and horizontal (□) modes are also shown.

We find that the frequency of vertically polarized resonant modes is significantly larger than horizontally polarized ones. This is due to a larger stiffness in compression than in shear.

APPENDIX C: FINITE DEPTH EFFECT ON THE DISPERSION RELATION

We consider here the dispersion relation of surface waves for a finite depth sample. As in the previous section, we assume that the displacement vanishes at $z=H$. There are two interesting limits. In the limit of large kH, we should recover the semi-infinite case ($\omega=\alpha\Gamma k^{-5/6}$) discussed in the body of the article. In the small kH limit, there is a waveguide cutoff. Importantly, here, the effect is not the gravity induced waveguide but a second one, due to the bottom boundary condition. We recall that the modes at vanishing k are nothing but the resonant modes derived previously. Thus, in the limit $kH\to 0$, the dispersion relation tends to $\omega=\alpha\Gamma H^{-5/6}$.

The full dispersion relations of transverse and sagittal modes are plotted on Fig. 10. They exhibit as expected a $(kH)^{5/6}$ asymptote and a cutoff frequency at $kH=0$. In the case of transverse waves, the cutoff resonant modes are polarized transversally (horizontal resonant modes). The cutoff frequencies are thus given by Eq. (B4). This in contrast with the sagittal modes, which present a wiggling dispersion relation at the approach of the cutoff frequency. As shown on Fig. 11, where the cutoff frequency is plotted as a function of the mode number, this is due to an irregular alternation of vertically polarized and horizontally polarized resonant modes. This is a strong feature of the present model.

[1] L. D. Landau and E. M. Lifshitz, *Theory of Elasticity*, 3rd ed. (Pergamon, New York, 1986).
[2] S. Douady, A. Manning, P. Hersen, H. Elbelrhiti, S. Protière, A. Daerr, and B. Kabbachi, Phys. Rev. Lett. **97**, 018002 (2006).
[3] H. Hertz, J. Reine Angew. Math. **92**, 156 (1882); see in [1].
[4] C. H. Liu and S. R. Nagel, Phys. Rev. Lett. **68**, 2301 (1992).
[5] X. Jia, C. Caroli, and B. Velicky, Phys. Rev. Lett. **82**, 1863 (1999).
[6] P. H. Brownell, Science **197**, 479 (1977); Sci. Am. **251**(6), 94 (1984); P. H. Brownell and R. D. Farley, J. Comp. Physiol. **131**, 23 (1979); **131**, 31 (1979).
[7] W. Sturzl, R. Kempter, and J. L. van Hemmen, Phys. Rev. Lett. **84**, 5668 (2000).
[8] A. Tanguy, J. P. Wittmer, F. Leonforte, and J. L. Barrat, Phys. Rev. B **66**, 174205 (2002).
[9] M. Wyart, L. E. Silbert, S. R. Nagel, and T. A. Witten, Phys. Rev. E **72**, 051306 (2005).
[10] Records of the song of dunes may be heard at http://www.pmmh.espci.fr/~andreotti/SongOfdunes.html
[11] M. Polo, in *The Description of the World*, edited by A. C. Mouleand Paul Pelliot (Routledge, London, 1938). Available online; see Ref. [10].
[12] C. Carus-Wilson, Nature (London) **44**, 322 (1891).
[13] F. J. Goldsmid, Geophys. J. **9**, 454 (1897).
[14] J. H. Poynting, Nature (London) **77**, 248 (1908).
[15] C. Carus-Wilson, Nature (London) **77**, 222 (1908).
[16] R. A. Bagnold, Proc. R. Soc. London, Ser. A **295**, 219 (1966).
[17] F. Nori, P. Sholtz, and M. Bretz, Sci. Am. **277**, 84 (1997).
[18] D. Goldsack, M. Leach, and C. Kilkenny, Nature (London) **386**, 29 (1997).
[19] B. Andreotti, Phys. Rev. Lett. **93**, 238001 (2004).
[20] M. Hunt (private communication);M. Hunt *et al.*,*Roaming Sand Dunes*, Minisymposium: Geophysical Fluid Dynamics, APS-DFD, Tampa, Nov. 2006.
[21] S. Douady, A. Manning, P. Hersen, H. Elbelrhiti, S. Protière, A. Daerr, and B. Kabbachi, Phys. Rev. Lett. **97**, 018002 (2006).
[22] B. Velicky and C. Caroli, Phys. Rev. E **65**, 021307 (2002).
[23] I. Goldhirsch and C. Goldenberg, Eur. Phys. J. E **9**, 245 (2002).
[24] J. Duffy and R. D. Mindlin, J. Appl. Mech. **24**, 585 (1957).
[25] P. J. Digby, J. Appl. Mech. **48**, 803 (1981).
[26] K. Walton, J. Mech. Phys. Solids **35**, 213 (1987).
[27] A. N. Norris and D. L. Johnson, J. Appl. Mech. **64**, 39 (1997).
[28] S. N. Domenico, Geophysics **42**, 1339 (1977).
[29] H. A. Makse, N. Gland, D. L. Johnson, and L. M. Schwartz, Phys. Rev. Lett. **83**, 5070 (1999); Phys. Rev. E **70**, 061302 (2004).
[30] Except maybe in the model case of 2D ordered packing of steel beads with a controlled weak polydispersity; see B. Gilles and C. Coste, Phys. Rev. Lett. **90**, 174302 (2003).
[31] D. Goddard, Proc. R. Soc. London, Ser. A **430**, 105 (1990).
[32] P.-G. Gennes, Europhys. Lett. **35**, 145 (1996).
[33] In writing this article, we became aware of a similar problem treated by another group in the special case $\mathcal{A}=0$ nonlinear elasticity; see V. E. Gusev, V. Aleshin, and V. Tournat, Phys. Rev. Lett. **96**, 214301 (2006).
[34] Y. Jiang and M. Liu, Phys. Rev. Lett. **91**, 144301 (2003); **93**, 148001 (2004); "A unified theroy of granular statics," report (unpublished).
[35] J. Boussinesq, C. R. Hebd. Seances Acad. Sci. **77**, 1521 (1873).
[36] We thank V. Gussev for pointing out the existence of these transverse modes.
[37] I. Agnoli *et al.*, in *Powders & Grains*, edited by R. Garcia-Rojo, H. J. Herrmann, and S. McNamaca (Balkema, Rotterdam, 2005), p. 313.